NSRRC - J05046 (2015)

ACS APPLIED MATERIALS & INTERFACES

Research Article

www.acsami.org

Synthesis of Thermoresponsive Amphiphilic Polyurethane Gel as a New Cell Printing Material near Body Temperature

Yi-Chun Tsai,[†] Suming Li,[‡] Shiaw-Guang Hu,[§] Wen-Chi Chang,[†] U-Ser Jeng,[∥] and Shan-hui Hsu*[,†]

[†]Institute of Polymer Science and Engineering, National Taiwan University, No. 1, Sec. 4 Roosevelt Road, Taipei 10617, Taiwan, R.O.C.

[‡]Institut Europeen des Membranes, Universite Montpellier, Montpellier 34090, France

[§]Department of Materials Science and Engineering, National Taiwan University of Science and Technology, Taipei 106, Taiwan, R.O.C.

[∥]National Synchrotron Radiation Research Center, Hsinchu City 300, Taiwan, R.O.C.

S *Supporting Information*

ABSTRACT: Waterborne polyurethane (PU) based on poly(ε-caprolactone) (PCL) diol and a second oligodiol containing amphiphilic blocks was synthesized in this study. The microstructure was characterized by dynamic light scattering (DLS), small-angle X-ray scattering (SAXS), and rheological measurement of the PU dispersion. The surface hydrophilicity measurement, infrared spectroscopy, wide-angle X-ray diffraction, mechanical and thermal analyses were conducted in solid state. It was observed that the presence of a small amount of amphiphilic blocks in the soft segment resulted in significant changes in microstructure. When 90 mol % PCL diol and 10 mol % amphiphilic blocks of poly(L-lactide)–poly(ethylene oxide) (PLLA–PEO) diol were used as the soft segment, the synthesized PU had a water contact angle of ~24° and degree of crystallinity of ~14%. The dispersion had a low viscosity below room temperature. As the temperature was raised to body temperature (37 °C), the dispersion rapidly (~170 s) underwent sol–gel transition with excellent gel modulus ($G' \approx 6.5$ kPa) in 20 min. PU dispersions with a solid content of 25–30% could be easily mixed with cells in sol state, extruded by a 3D printer, and deposited layer by layer as a gel. Cells remained alive and proliferating in the printed hydrogel scaffold. We expect that the development of novel thermoresponsive PU system can be used as smart injectable hydrogel and applied as a new type of bio-3D printing ink.

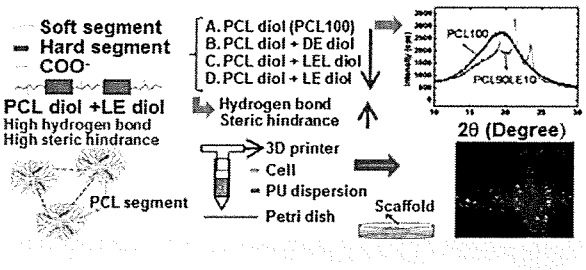

KEYWORDS: *waterborne polyurethane, amphiphilic block copolymer, small-angle X-ray scattering (SAXS), hydrogel, 3D-printing ink*

1. INTRODUCTION

Polyurethane (PU) elastomers are linearly segmented polymers consisting of a relatively long and flexible component contributed by the oligodiol (soft segment) and a relatively rigid component derived from a diisocyanate and a chain extender (hard segment). Waterborne PU is often synthesized by introducing an ionic component that transforms PU to an ionomer and make it dispersed in water.[1,2] Water-based PU has several advantages over the conventional PU, e.g., the process is eco-friendly and nonflammable; thus, it is used in a broad range of industry domains such as painting, adhesive, leather, and textiles. In the biomedical field, it serves as wound dressings, surgical sutures, and drug carriers.[3−6]

An amphiphilic block copolymer is an additive copolymer that contains hydrophilic and hydrophobic blocks. It can self-assemble into various structures in selective solvents because of the thermodynamic incompatibility between the blocks. Polylactide–poly(ethylene oxide) (PEO) copolymer is a typical amphiphilic copolymer that can be applied in medicine. The poly(L-lactide) (PLLA) or poly(D,L-lactide) (PDLLA) block is biodegradable and hydrophobic, whereas the PEO block is soluble in water and has good biocompatibility. Related products have been approved by the U.S. Food and Drug Administration for use in the human body.[7−10]

The volume ratio of PEO in the polylactide-PEO block copolymer critically determines its morphology in the solvent, which can be in the form of micelles, vesicles, microspheres, or hydrogel.[11−13] The hydrophilicity and flexibility of PLLA–PEO and PDLLA–PEO copolymer are improved over that of the homopolymer PLLA or PDLLA.[14] In contrast to polylactide, poly(ε-caprolactone) (PCL) degrades more slowly, but the degradation time can be shortened by making copolymers with the other polymers. For example, the PLLA–PCL copolymer is tougher and degrades faster than pure PCL.[15] Linking amphiphilic blocks by isocyanate reaction could retain their self-assembly and self-emulsification properties;[16,17] however, the resulting copolymers had relatively low molecular weight and elasticity in general. We have previously synthesized PU

Received: February 27, 2015
Accepted: November 26, 2015
Published: December 9, 2015

 © 2015 American Chemical Society

DOI: 10.1021/acsami.5b10697
ACS Appl. Mater. Interfaces 2015, 7, 27613−27623

anionomeric nanoparticles (NPs, ~40 nm) dispersed in water using PCL diol as the soft segment.[18] All the previous PUs based on PCL–PEO or PLLA–PEO were solvent-borne.[19] Water-dispersed high-molecular-weight PU employing PLLA–PEO or PDLLA–PEO blocks has not been reported so far.

3D printing has emerged as a new biofabrication technique. Materials for biomedical 3D printing can be either natural or synthetic polymers. Natural polymers such as gelatin, collagen, alginate, and chitosan are commonly used, but they often need cross-linkers that may be cytotoxic.[20] Synthetic biodegradable polyesters such as polylactic acid (PLA) and polyglycolic acid (PGA) require high temperature or organic solvent for processing,[21] which is not suitable for cell printing. Waterborne PCL-based anionic NPs can only be printed at a temperament below −20 °C, which is also not possible for cell printing.[22] In this study, we employed PCL diol as the major soft segment while replacing 10 mol % soft segment by the oligodiol of amphiphilic blocks (PLLA–PEO diblock, LE, or PDLLA–PEO diblock, DE) or substituting 20 mol % soft segment by PDLLA–PEO-PLLA triblock, LEL, oligodiol to prepare the new series of waterborne PU NPs. We expected that introducing amphiphilic blocks of a small fraction into PU structure may cause a significant change in the physicochemical properties and generate new functions. We then carried out dynamic light scattering (DLS), small-angle X-ray scattering (SAXS), wide-angle X-ray diffraction (XRD), and mechanical, thermal, and rheological analyses to portray the mechanism accounting for the physicochemical changes of PU-containing amphiphilic blocks.[23] We demonstrated that the water-based dispersion of PU NPs containing amphiphilic blocks had low viscosity (~3 Pa·s) below room temperature but could form gel rapidly with gel modulus approaching 6500 Pa as the temperature was raised to body temperature without the need of cross-linkers. This thermoresponsive fast gelation allowed the new waterborne PU to be printed and deposited layer by layer. Besides, the good mechanical properties of PU may protect cells from shear damage upon printing. We therefore suggested that the smart PU NP dispersion may serve as a novel type of low-viscosity 3D-cell-printing ink.

2. EXPERIMENTAL SECTION

2.1. Synthesis of Block Oligodiols. Three types of block oligodiols were synthesized for use in the PU reaction, as shown in Figure 1. They were poly(L-lactide-*co*-poly(ethylene oxide)) (LE) diol, poly(D-lactide-*co*-poly(ethylene oxide)) (DE) oxide, and poly(L-lactide-*co*-poly(ethylene oxide)-*co*-L-lactide) (LEL) diol.

LE diol (M_n= 3387) and DE diol (M_n= 3297) were prepared as described below. L(or D)-Lactide was obtained from Purac, and monomethoxy poly(ethylene oxide) (mPEO, Mn= 2000) was supplied by Fluka. L(or D)-Lactide and mPEO were added into a flask. The molar ratio of ethylene oxide to lactate repeat units (EO/LA) was 45/19 for LE and 45/18 for DE. Zinc lactate (0.1 wt %) was then added as the catalyst. After degassing, the flask was sealed under vacuum, and the polymerization was conducted at 140 °C. After 7 days, the product was recovered by dissolution in dichloromethane (CH_2Cl_2) and precipitation in diethyl ether. Finally, the product was dried under the vacuum.[24]

LEL diol (M_n= 2200) was prepared as described below. Poly(ethylene oxide) diol (PEO, M_n= 1000) was supplied by Hanaka (Japan). Tin(II)2-ethylhexanoate (T-9) was from Alfa Aesar. PEO was dried in a vacuum oven at 150 °C for 3 days. L-Lactide and PEO were placed in a 50 mL round-bottomed flask equipped with a stirrer. The reaction mixture was heated to 130 °C with stirring under N_2, and 0.05 wt % T-9 was then added. The mixture was stirred for 10 h at 130 °C. The final product obtained was dissolved into CH_2Cl_2 and

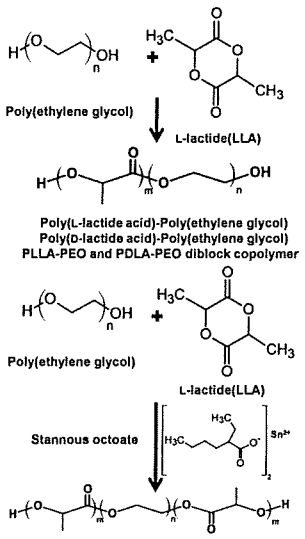

Figure 1. Synthesis process for the diblock copolymers LE and DE and triblock copolymer LEL.

cooled to 25 °C. Subsequently, the products were extracted with a cold solvent mixture of methanol and *n*-hexane. Finally, the product was dried in a vacuum oven at 40 °C for 3 days.[25]

2.2. Synthesis of Waterborne PU. Raw materials included isophorone diisocyanate (IPDI, from Evonik Degussa GmbH), ethylenediamine (EDA, from Tedia), 2,2-bis(hydroxymethyl)propionic acid (DMPA, from Aldrich), triethylamine (TEA, from RDH), methyl ethyl ketone (MEK, from J.T. Baker), and T-9.

Waterborne PU was synthesized by a two-step reaction process previous developed.[18] The chemical structures of waterborne PU are shown in Figure 2. A 250 mL round-bottomed, four-necked separable flask with a mechanical stirrer, thermometer, condenser with a drying tube, and N_2 inlet was used as reactor. There were four kinds of oligodiols used in synthesis including poly(ε-caprolactone) (PCL) diol, LE diblock diol, DE diblock diol, and LEL triblock diol. The reaction was carried out in a constant temperature oil bath. IPDI and T-9 were added to the stirred oligodiols put into the dried flask and stirred at prepolymerization temperature for 3 h (180 rpm). DMPA and a limited amount of MEK were subsequently added and reacted at 70 °C for 1 h (180 rpm). The mixture was cooled down to 50 °C, and TEA was added and stirred for 30 min. A solution of EDA in deionized water was added to the prepolymer dispersion, and the mixture was vigorously stirred for 30 min. The stoichiometric ratio of IPDI/oligodiols/DMPA/EDA/TEA was 3.52:1:1:1.52:1.The residual MEK and TEA was removed from the mixture by vacuum distillation to obtain a PU water dispersion with a solid content of about 30%. In the chemical structure of PU, the weight percent of soft segment was >65%. The PU dispersion was characterized or cast onto Teflon plates to create films (1 mm thick) for bulk characterization.

2.3. Physicochemical Characterization. The hydrodynamic size and zeta potential of PU NPs were measured by a Delsa Nano C Particle Analyzer using the principles of DLS and electrophoretic light scattering. Before the measurement, the PU dispersion was diluted with distilled water to 3000 ppm.

The surface water contact angle of cast films was measured by a contact angle analyzer (FTA-1000 B, First Ten Angstrom Company, USA) at 25 °C. A water droplet of 5 μL was used for each measurement. Values obtained from different locations of the films were averaged. The surface chemistry of PU films was characterized by the attenuated total reflection-infrared (ATR-IR) spectroscopy. The spectra were collected by a spectrophotometer (Spectrum 100, PerkinElmer, Waltham, MA, USA) in the wavenumber range of 4000–650 cm^{-1}.

The tensile properties were measured using a universal testing instrument (HT-8504, Hung Ta Co., Taiwan) following the ASTM

DOI: 10.1021/acsami.5b10697
ACS Appl. Mater. Interfaces 2015, 7, 27613–27623

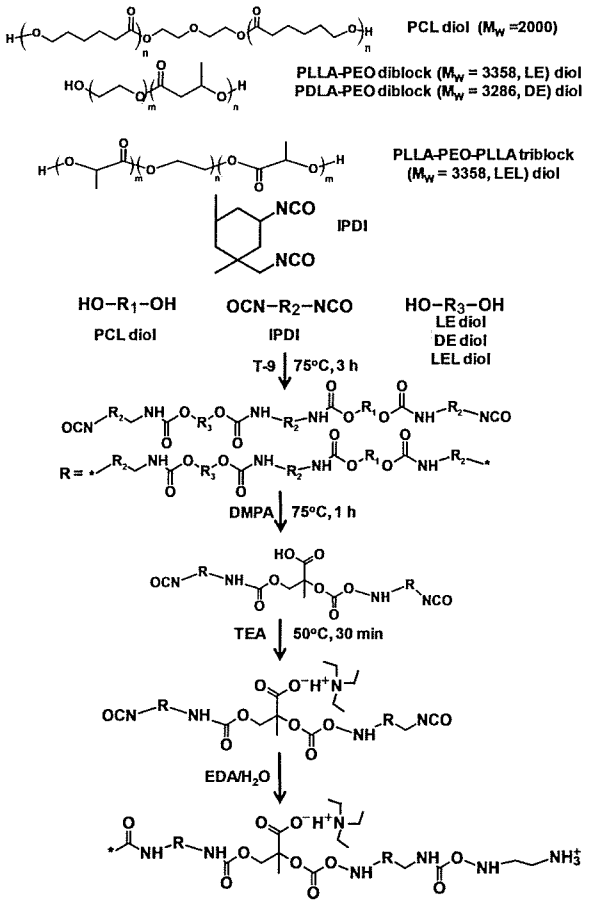

Figure 2. Synthetic process for PU, employing amphiphilic blocks as the soft segment.

standard protocol (ASTMD638.10). The specimens were in the size of 25 mm (length) × 5 mm (width) × 1 mm (thickness). Values were obtained at a stretching rate of 100 mm min^{-1} for elastomers.

The thermogravimetric analysis (TGA) was carried out with a thermogravimetric analyzer (TA Instrument). Each sample (5 mg) was placed in an alumina crucible and heated at a rate of 10 °C per min under N_2. The glass transition temperature (T_g) and melting temperature (T_m) were obtained by a differential scanning calorimeter (DSC, PerkinElmer Pyris 6, USA). The PU film was pressed in an aluminum sample pan. The operating temperature was from −70 to 150 °C with a heating rate of 10 °C per min. The weight-average molecular weight (M_w) was determined by gel permeation chromatography (GPC, Waters, USA) in *N*-methyl-2-pyrrolidone using polystyrene as standard.

The PU dispersion was first gelled at 37 °C for 48 h. The swelling test was carried out on cylindrical gels (height 1.0 cm; diameter 1.5 cm). The samples were lyophilized for 24 h (W_i) after removal of excess water on the surface (W_w). The percentage of swelling ratio was calculated by the following formula: swelling ratio (%) = $[(W_w - W_i)/W_i] \times 100\%$

2.4. XRD and SAXS Experiments. The PU film was cropped to the appropriate size and examined by XRD for crystallization characteristics of the material. The equipment was operated at the power of 2 kW and measurement was made in the range of 2θ =10−30° (where θ is the scattering angle). The degree of crystallinity was calculated by the integrated area of the characteristic crystalline peaks over the total integrated area.

The microstructures of PU NPs in dispersion were investigated by SAXS at the beamline 23A of National Synchrotron Radiation Research Center (Hsinchu, Taiwan). The photon energy was at about 10 keV. For anaylsis by the Guinier method ($\ln I = \ln I_0 - ((q^2Rg^2)/3)$), a plot of the logarithm of the intensity I ($\log I$) versus the square of scattering vector q^2 was obtained. The radius of gyration (R_g) was estimated based on the Guinier analysis under the circumstance $qR_g < 1.3$. The fractal dimension (d_f) was obtained as the negative slope of the $\log I$ versus $\log q$ plot.

2.5. Rheological Studies. The rheological properties of PU dispersions were determined using a rheometer (RS-S, TA Instruments). A cone and plate geometry with a frequency of 1 Hz and a deformation of 1% was used. The dynamic storage modulus (G') and dynamic loss modulus (G'') were measured against time. Sol−gel transition was defined as the point where $G' = G''$.

2.6. Cell Culture. Human umbilical cord derived mesenchymal stem cells (MSCs) were supplied by BIONET Corp (Taipei, Taiwan). MSCs were cultured in T150 tissue-culture flasks (Falcon, BD Biosciences). The basal medium consisted of low-glucose Dulbecco's modified Eagle medium (LG-DMEM), 10% fetal bovine serum (FBS; SAFC Biosciences, USA), 1% penicillin−streptomycin (Caisson, USA), and 0.4% gentamicin (Gibco). Cells were incubated in a humidified incubator with 5% CO_2 at 37 °C. Cells at the eighth passage were used in this study. Before the 3D printing, cells were stained with a red fluorescent dye PKH26 (Sigma).

2.7. 3D Printing of PU Dispersion. PCL90LE10 (30%) was heated at 37 °C for 30 min. To perform the pretest, the near-gelling emulsion was extruded via a needle manually to prepare the fibers. The needle had a size of 26G (inner diameter, 260 μm, and outer diameter, 463.6 μm), and the emulsion was injected at a volumetric flow rate of 5.56 μL/s. Five to seven parallel arrays of fibers were injected to compose the first layer. The second layer was deposited at an angle of 90° relative to the first layer. The constructs were placed in an incubator at 37 °C. On the basis of our observation, the above procedure may be repeated 40 times to produce stacking layers .

PCL90LE10 (30%) was then mixed with cells (human MSCs) so that 1 mL of PCL90LE10 contained ~2 × 10^6 cells. The near-gelling emulsion of PCL90LE10 was tested as the 3D-printing ink by a fused deposition manufacturing (FDM) platform.[26] Hydrogel scaffolds were prepared in 3 cm × 3 cm square with 2 mm thickness. The syringe diameter was 260 μm. The stacking pattern of fibers was 0°/90°. The gas pressure was 241−275 kPa, and the volume flow rate was 1.67 μL per second. To print cell-containing hydrogel, PCL90LE10 (25−30%) dispersion (2 mL) was mixed with human MSCs at 25 °C and heated at 37 °C for 10 min before loading into the needle of the 3D printer. After printing, cell-laden constructs were cultured in 3 mL of medium and incubated in a humidified incubator with 5% CO_2 at 37 °C. Cell morphology was observed by fluorescence microscope after 0, 1, 2, 3, and 7 days.

2.8. Cell Viability and Proliferation. Cell proliferation was measured by the MTT assay. At the specified time points, the cell-laden constructs were washed in phosphate-buffered saline (PBS), and 200 μL of 0.1 mg/mL tetrazolium dye (Sigma-Aldrich) was added, followed by incubation for 4 h at 37 °C. At the end of the incubation period, the tetrazolium dye was removed. The purple formazan formed was dissolved in ethanol and read at 570 nm using a microplate reader (SpectraMax M5, USA). The optical density was normalized to that of the control cells (0 days before seeding). For statistical analysis, data from multiple samples were collected in each independent experiment. The reproducibility was confirmed in at least three experiments. The statistical significance difference was evaluated by one-way analysis of variance; p values < 0.05 were considered statistically significant.

Before immunohistochemical staining, the samples were washed in PBS buffer (pH 7.2−7.4). The samples were then blocked for an hour using 2% bovine serum albumin (BSA; molecular weight, 62 kDa) before incubation with anti-Ki67 antibody (1:100; GeneTex) at 4 °C for 24 h and then the secondary antibody (1:500; GeneTex) at 4 °C for 24 h.

3. RESULTS

3.1. Characterization of PU NPs and Physicochemical Characterization. The hydrodynamic diameter (D_h) of each

DOI: 10.1021/acsami.5b10697
ACS Appl. Mater. Interfaces 2015, 7, 27613−27623

Table 1. Abbreviations and Properties of PU Prepared in This Study

	molar percent of the PU soft segment (%)				DLS			
abbreviation of PU	PCL	PLLA	PDLA	PEO	hydrodynamic diameter (D_h, nm)	zeta potential (mV)	complex viscosity (Pa·s)	contact angle (°)
PCL100	100	0	0	0	39.30 ± 0.9	−57.0 ± 2.1	2.16	83.04 ± 1.8
PCL90LE10	90	2.969	0	7.031	26.85 ± 0.9	−37.26 ± 1.8	3.88	23.51 ± 2.3
PCL90DE10	90	0	2.857	7.143	37.07 ± 1.1	−36.24 ± 2.7	2.17	55.83 ± 3.7
PCL80LEL20	80	8.421	0	11.579	31.93 ± 0.5	−29.3 ± 0.6	2.23	72.50 ± 1.4

type of PU NPs is listed in Table 1. PCL100 NPs had the largest D_h of 39.3 nm. Replacing a part of soft segment by amphiphilic blocks decreased D_h values to 26–37 nm. Particularly, PCL90LE10 NPs showed the smallest D_h value. The zeta potential of various PU NPs was between −29 and −58 mV.

The surface water contact angle of PU films cast from the PU NP dispersion is demonstrated in Table 1. PCL100 films showed the largest contact angle of 83.0°. Substituting the soft segment with a small fraction of amphiphilic blocks decreased the contact angle values to 23–73°. Among the films, PCL90LE10 had the lowest contact angle of 23.5°. Therefore, PCL90LE10 films were the most hydrophilic among all samples.

ATR-IR spectra of the PU films are shown in Figure 3A. The stretching bands at 2260–2280 cm^{-1} (–NCO group) and

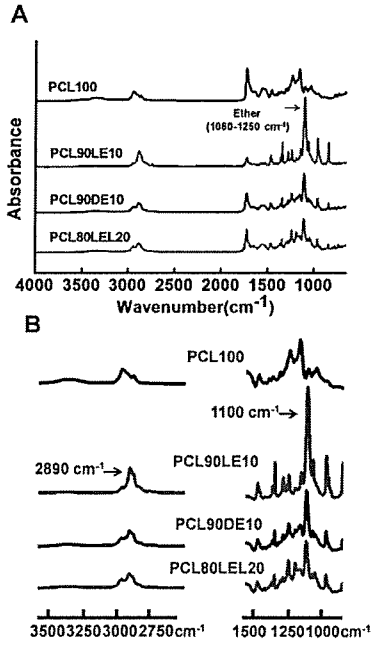

Figure 3. (A) ATR-IR spectra of the PU. (B) Enlarged ATR-IR spectra for the bands of C–H and C–O–C vibrations.

at 3200–3600 cm^{-1} (O–H group) were absent in all sample films, confirming that the diisocyanate, oligodiols, and chain extenders had completely reacted during the PU synthesis. The absorption peaks at 3350 cm^{-1}(N–H group) and 1730 cm^{-1} (C=O group in urethane and ester) observed for all PU films and were the strongest in PCL100 samples. The peak at 1060–1250 cm^{-1} (C–O–C) was attributed to the symmetric and asymmetric stretching vibration of ester in all samples. The band in 2860–2900 cm^{-1} (methylene) was attributed to the symmetric and asymmetric stretching of the methylene group. Enlarged ATR-IR spectra in the range of 2700–3600 and 1000–1500 cm^{-1} are shown in Figure 3B. For PUs containing amphiphilic blocks, the absorption intensity at 1100 cm^{-1} increased, which was associated with the stretching vibration of C–O–C (ether) in the EO block. The characteristic band at 2890 cm^{-1} originated from the stretching of CH_2 groups in EO.[27,28] PCL90LE10 revealed the highest absorption peaks at 1100 and 2890 cm^{-1}, indicating that PCL90LE10 surface was enriched with the EO block. The latter finding was consistent with the excellent surface hydrophilicity (low contact angle) observed for this sample.

3.2. Mechanical and Thermal Properties of PU. The tensile stress–strain curves of various PU films are shown in Figure 4A. The molecular weight, Young's modulus, 100%

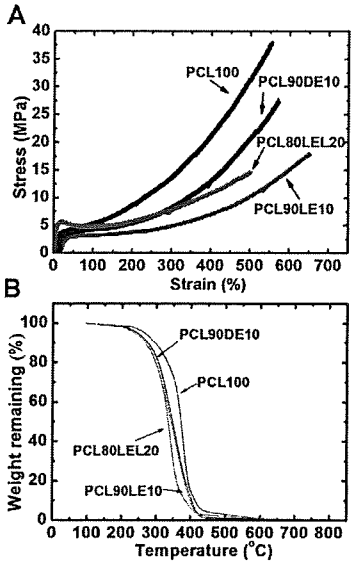

Figure 4. (A) Typical stress–strain curves for various PU. (B) TGA curves of PU.

modulus, tensile strength, and elongation obtained from the curves are summarized in Table 2. Among the films, PCL100 had the largest molecular weight and tensile strength (~35 MPa). The higher molecular weight of PCL100 was ascribed to the higher reactivity of the PCL oligodiol compared to the amphiphilic blocks. PCL80LEL20 had the largest Young's modulus (~157 MPa) but the smallest tensile strength (~15 MPa), probably because of the higher LA contents of this polymer. The tensile strength of PCL90LE10 and PCL90DE10 (~19–25 MPa) fell between those of PCL100 and PCL80LEL20. All films showed the maximum elongation over 500%, indicating the elastomeric nature of all PU samples. The tensile strength was well-correlated with the molecular weight.

DOI: 10.1021/acsami.5b10697
ACS Appl. Mater. Interfaces 2015, 7, 27613–27623

Table 2. Molecular Weight of PU and the Tensile Properties (25°C) of PU Films

	molecular weight (M_w, Da)	Young's modulus (MPa)	100% modulus (MPa)	tensile strength (MPa)	elongation at break (%)
PCL100	165354	30.9 ± 7.9	5.30 ± 0.1	34.9 ± 3.1	535.5 ± 19
PCL90LE10	72063	18.6 ± 2.8	3.16 ± 0.3	18.8 ± 1.2	650.6 ± 10
PCL90DE10	84529	15.7 ± 1.5	4.13 ± 0.2	25.2 ± 1.5	573.3 ± 2.3
PCL80LEL20	54961	15.7 ± 2.2	4.77 ± 0.3	14.7 ± 3.7	500.0 ± 14

Table 3. TGA Measurement of T_{onset} and T_d, DSC Measurement of T_g and T_m, and XRD Calculation of the Degree of Crystallinity (X_c) in PU Films

	TGA		DSC		XRD peaks			
	T_{onset} (°C)	T_d (°C)	T_g (°C)	T_m (°C)	PLA (2θ = 16.7°, %)	PEO (2θ = 19.2°, %)	PCL (2θ = 21.3°, %)	PCL (2θ = 23.5°, %)
PCL 100	266.0	372.2	−53.06	NA[a]	NA	NA	0	0
PCL90LE10	236.4	343.5	−51.57	60.78	0	0.99	8.35	4.69
PCL90DE10	243.9	347.7	−51.59	55.59	0	0.55	0.89	1.62
PCL80LEL20	231.5	334.8	−47.74	NA	0.42	0.24	3.75	1.28

[a]NA = Not applicable.

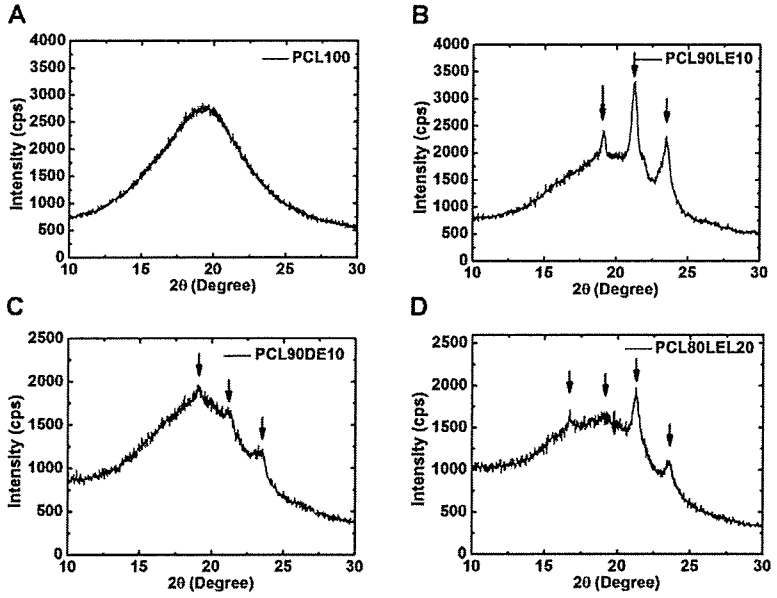

Figure 5. Typical X-ray diffraction patterns of PU: (A) PCL100, (B) PCL90LE10, (C) PCL90DE10, and (D) PCL80LEL20.

TGA curves of PU are shown in Figure 4B. The onset decomposition temperature (T_{onset}) and thermal decomposition temperature (T_d) are listed in Table 3. PCL100 had the highest T_{onset} and T_d, whereas PCL80LEL20 had the lowest T_{onset} and T_d. The thermal stability of the materials ranked in the order of PCL100 > PCL90DE10> PCL90LE10 > PCL80LEL20. The glass transition temperature (T_g) and melting temperature (T_m) of PU are also shown in Table 3. PCL100 had the smallest T_g, whereas PCL80LEL20 had the highest T_g. On the basis of the above analyses, the degree of microphase separation was the greatest in PCL100, followed by PCL90DE10 and PCL90LE10, and was the smallest in PCL80LEL20.

3.3. X-ray Diffraction Analysis. XRD profiles are displayed in Figure 5. PCL100 revealed a broad band without any characteristic peak, i.e., it was amorphous in nature. In contrast, PUs introduced with amphiphilic blocks as soft segments showed characteristic peaks of crystallization. Peaks with the locations at 2θ = 16.7 and 19.2° were associated with the LA and EO block, respectively. Peaks with the locations at 2θ = 21.1 and 23.3° were associated with PCL. The degree of crystallinity for PU films is listed in Table 3. PCL90LE10 had the largest degree of crystallinity (~14%). Moreover, the crystalline EO block in PCL90DE10 and PCL90LE10 may account for their microphase separation in comparison with the less-crystalline EO block in PCL80LEL20.

3.4. Macroscopic Observation of PU Gelation. The prepared PU was stored in a refrigerator (10 °C) before investigation of the gelation behavior in room temperature over a period of time. Slow gelation at an average temperature of 26 °C was observed (Figure S1). PCL90LE10 was gel-like on the fifth day, whereas PCL90DE10 formed a viscous fluid (semigel-like) on the fifth day and was gel-like on the seventh day. PCL80LEL20 showed a tendency of gelation similar to that of PCL90DE10. The above gross observation revealed that the hydrophilicity (hydration) and degree of crystallinity might contribute to gelation. PCL90LE10 was subjected to further analyses because of its favorable gelation time and low percentage of PEO segments. PEO is soluble and metabolized

DOI: 10.1021/acsami.5b10697
ACS Appl. Mater. Interfaces 2015, 7, 27613−27623

at low molecular weight but is not a biodegradable segment. All materials had a swelling ratio ~200%.

3.5. Small Angle X-ray Scattering Analysis. The SAXS profile of PCL90LE10 is shown in Figure 6. The curve

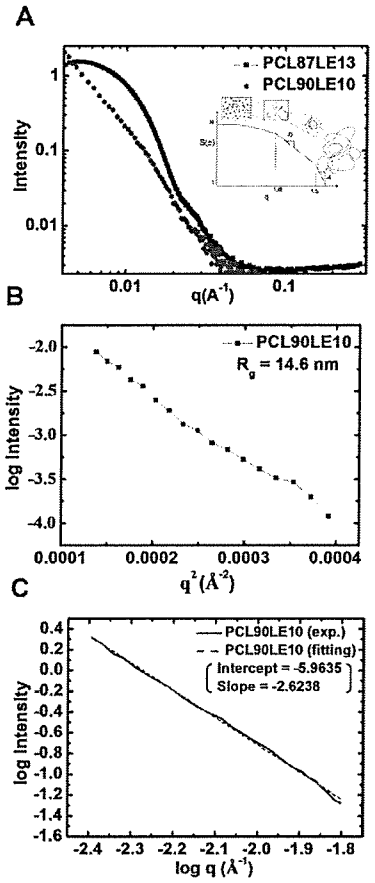

Figure 6. SAXS profiles of PCL87LE13 and PCL90LE10 PU NP dispersion. (A) Intensity plots for PCL87LE13 and PCL90LE10. (B) Plot of log(intensity) versus q to obtain the value of R_g. (C) Plot of log(intensity) versus log q to obtain the value of fractal dimension.

measured at 24 h after synthesis (Figure 6A) revealed a relatively plateau region for scattering intensity in the low q region (0.001–0.01 Å^{-1}). For samples measured after gelling, the intensity dropped rapidly and the slope was steep even in low q region (Figure 5B). Because the aggregation behavior of PCL90LE10 was time-dependent, two analytical methods were applied to account for the time dependency. For nonaggregated PCL90LE10, the Guinier method for qR_g below 1.3 that ignored the change of refractive index with concentration was appropriate. The results of Guinier analysis showed an R_g of 14.6 nm. Additionally, as the ratio of LE got higher (PCL87LE13), the value of R_g increased to 17.8 nm (Figure S2). For aggregated PCL90LE10, fractal analysis was used on q values ranging from 0.00404 to 0.01577 where a slope of −2.62 was obtained, as shown in Figure 6C. On the basis of the literature,[29] the fractal dimension of PCL90LE10 gel was 2.62, a value close to that reported for percolation clusters.[30]

3.6. Rheological Properties. The rheological properties of PCL90LE10 at different temperatures are shown in Figure 7. The approximate equilibrium gel modulus is listed in Table 4.

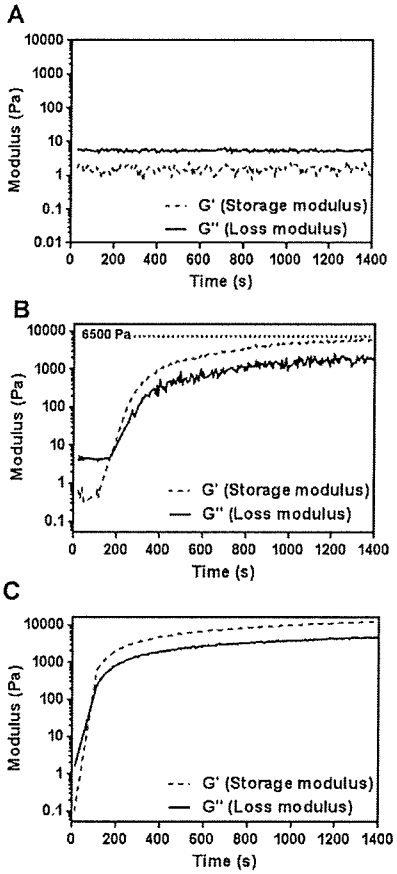

Figure 7. Time-dependent changes of storage modulus (G') and loss modulus (G'') of PCL90LE10 upon exposure to various temperatures: (A) 25 °C, (B) 37 °C, and (C) 50 °C.

Table 4. Gelation Time of PCL90LE10 NP Dispersion (Solid Content 30%), Approximate G' of the Cured Gel at Various Temperatures[a]

	PCL90LE10	
temp (°C)	gelation time (s)	G' (Pa)
25 (stable)	NA	NA
37	169	6590
50	84	12242

[a]The observation time was about 25 min.

When PCL90LE10 was placed at 25 °C, the moduli G' and G'' did not change significantly with time. When the temperature was maintained at 37 °C, G' and G'' crossed over after 169 s. The elastic modulus (G') reached ~6500 Pa in 20 min. When the temperature was controlled at 50 °C, PCL90LE10 gelled after 84 s, and G' reached ~12 000 Pa in 20 min. These results indicated that PCL90LE10 gelled rather slowly below 25 °C, but the gelation was obviously accelerated at higher temperatures.

3.7. PU as a Possible New Type of Thermoresponsive 3D-Printing Ink. PCL90LE10 with a solid content 30% was taken from the refrigerator and placed at 37 °C for 10 min and then loaded in a needle (26G, 260 μm). Gel formed after injection through the needle. When kept at 37 °C, the gel could be deposited layer by layer, as shown in Figure 8A,B. The gel was further printed at 37 °C using the 3D printer (FDM system).

DOI: 10.1021/acsami.5b10697
ACS Appl. Mater. Interfaces 2015, 7, 27613–27623

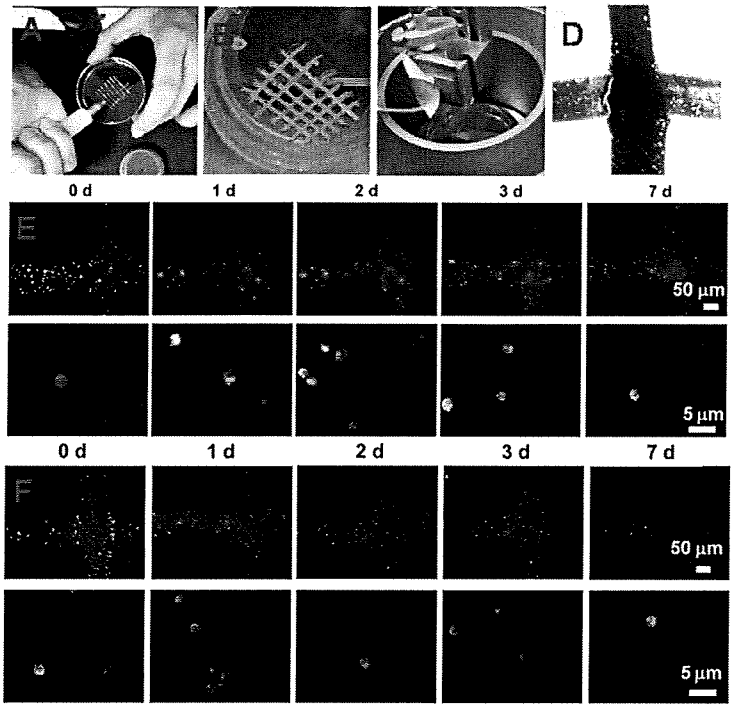

Figure 8. Thermally induced gelling of needle-injected PCL90LE10 fibers and the layer-by-layer stacking of the deposited fibers: (A) 40-layer stacking fibers fabricated by manual injection, (B) construct formed, (C) 3D printing by a self-designed FDM platform, (D) 3D-printed fibers (two layers for cell visualization by the optical microscope), (E) cells in the 3D-printed fibers (30% solid content), and (F) cells in the 3D printed fibers (25% solid content) during a period of 7 days.

As shown in Figure 8C,D, PCL90LE could be successfully printed. The initial viscosity was ~3 Pa·s (Table 1), and the viscosity for printing was ~8 Pa·s.

PCL90LE10 (30%) was then mixed with cells (human MSCs, ~ 2×10^6 cells/ml) at 25 °C and heated at 37 °C for 10 min before loading into the needle of the 3D printer. Figure 8E shows that the embedded cells may be printed with the gel. Cells remained alive during a period of 7 days and could proliferate after 48 h. Gel with a lower solid content (25%) was also printed. Cells proliferated better in the more dilute gel (Figure 8F). These results supported the idea that PCL90LE sol–gel may be applied as a possible cell-printing ink because of the thermoresponsiveness near 37 °C. Cell viability evaluated by the MTT assay is shown in Figure 9A. The cell viability in 25% PCL90LE10 gel was ~5% after 1 day, but increased significantly afterward, and reached ~160% of the initial value after 7 days, indicating cell proliferation during the period. The cell viability in 30% PCL90LE10 gel was ~25% after 1 day, increased to ~5% at 2 days, but decreased to ~5% after 7 days. The images of Ki67 staining showing the proliferating status of MSCs are presented in Figure 9B. On the basis of the fluorescent images, the number of proliferating cells increased during a period of 7 days in 25% PCL90LE10 gel. In contrast, MSCs in 30% PCL90LE10 showed a decrease of live cells from 2 to 7 days. The percentage of proliferating cells quantified on the basis of Ki67 staining in Figure 9B during a period of 7 days is shown in Figure 9C. The percentage of Ki67 positive cells in 25 and 30% PCL90LE10 gels were both ~86% at 0 h but decreased significantly to ~38% after 1 day. After 3 days, the percent positive cells kept decreasing in 30% PCL90LE10 gel, but increased in 25% PCL90LE10 gel and reached ~88% after 7 days. These data were consistent with those obtained by the MTT assay. The good cell survival in 25% PCL90LE10 gel may have led to the cell proliferation after 3 days.

4. DISCUSSION

The waterborne PU NPs prepared in this study had small hydrodynamic sizes and low zeta potentials, suggesting that all formulas may be stably dispersed in water. The negative charge was attributed to the COO^- functional group in the hard segment. When the diblock or triblock copolymer diol replaced a small part of PCL diol, the NP size became smaller, and the zeta potential increased (less negative). Besides, the surface contact angle of the cast films decreased. These changes may be associated with the introduction of more hydrophilic LA and EO blocks in the chemical structure of the PU. EO may form hydrogen bonding with water. When the PU contacts water, the hydrophobic $-CH_2-CH_2$ may turn inside, and the hydrophilic C–O–C may orient outside,[31] increasing the hydrophilicity of the NP and cast films. The structure of PCL90LE10 may especially favor the orientation of C–O–C to the surface, causing the low contact angle of the film. This surface orientation of C–O–C was confirmed by ATR-IR. The ATR-IR spectra of PU did not show any peak around 2260–2280 cm^{-1} (NCO) or 3200–3600 cm^{-1} (OH), indicating that the synthesis reaction was complete. In contrast, an evident peak was observed near 1060–1250 cm^{-1} (asymmetric stretching C–O–C) for PUs containing amphiphilic blocks. In particular, PCL90LE10 showed significant absorption near 1060–1250 cm^{-1}. These data, together with the low contact angle of PCL90LE10 films, suggested that the PCL90LE10 surface had the most exposed EO blocks.

DOI: 10.1021/acsami.5b10697
ACS Appl. Mater. Interfaces 2015, 7, 27613–27623

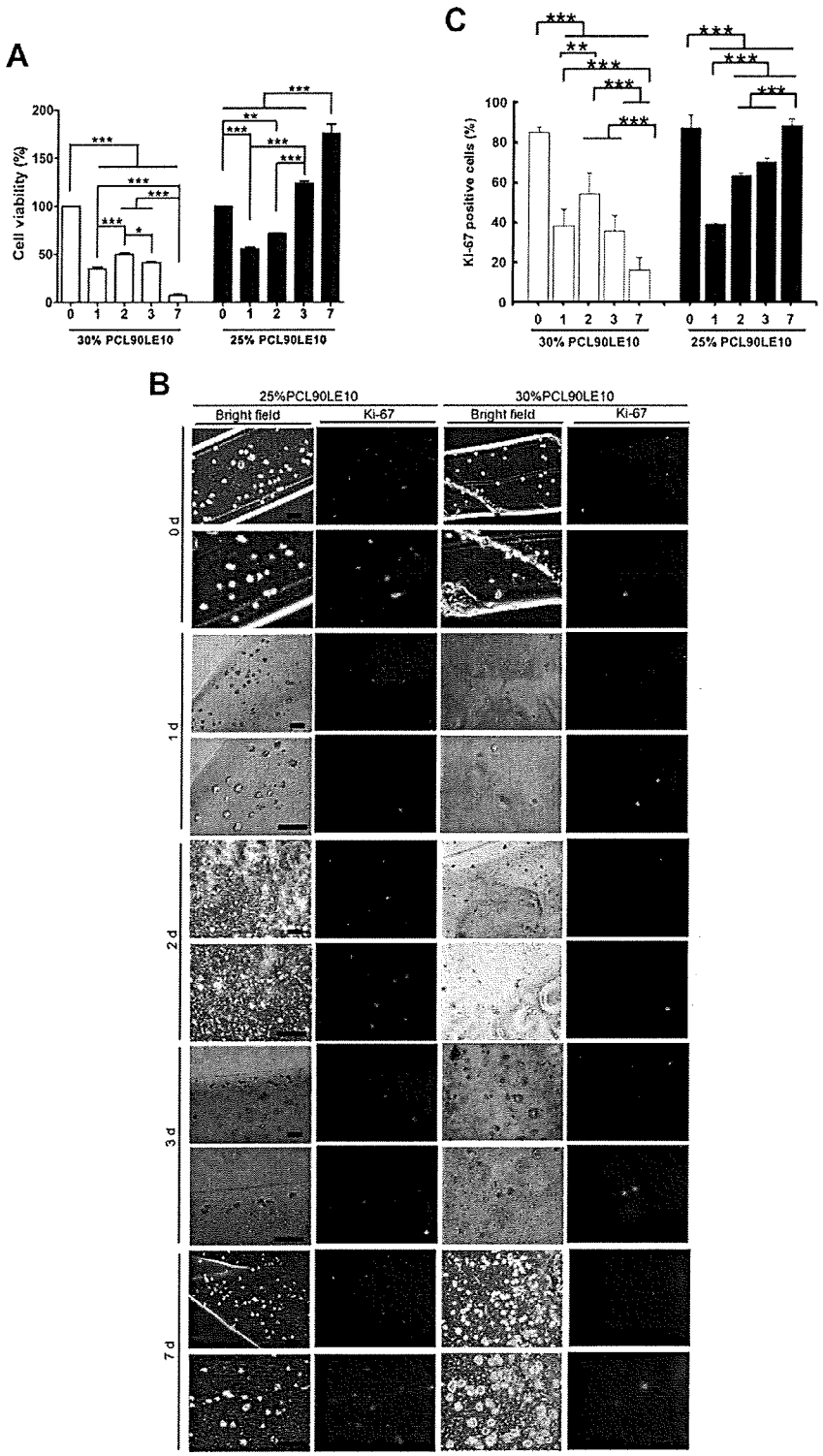

Figure 9. Viability and proliferation of cells cultured in PCL90LE10 gel with 25 and 30% solid content. (A) MTT assay showing the viability of cells at 0, 1, 2, 3, and 7 days. The absorbance value was measured at 570 nm using a microreader and normalized to the absorbance value for each concentration of PU gel at 0 days. The statistical significance difference was evaluated by using one-way analysis of variance. (B) Immunohistochemical staining for Ki67 protein showing the proliferating cells at 0, 1, 2, 3, and 7 days. Scale bar represents 100 μm. (C) Percentage of K_i-67 positive cells quantified on the basis of *Ki*67 staining. *, $p < 0.05$; **, $p < 0.01$; and ***, $p < 0.001$.

DOI: 10.1021/acsami.5b10697
ACS Appl. Mater. Interfaces 2015, 7, 27613−27623

PCL100 had the best mechanical and thermal properties. This was because of the more abundant ester group in PCL100.[32] The polyester-type PU may form hydrogen bonds more readily than the polyether-type PU, which contributes to greater tensile properties. Introducing LA/EO-containing block copolymer could increase T_g. This may be ascribed to the crystallization of soft segment.[33] It was interesting to note that PCL80LEL20 had the largest Young's modulus and the smallest elongation. The low elongation was associated with the higher content of LA. The presence of LA probably contributed to crystallinity and low ductility.

PU based on 100% PCL diol (PCL100) demonstrated no crystalline peak in XRD. A previous study showed that introduction of 20% PLLA diol (PCL80LL20) may cause steric hindrance and secondary force, leading to crystallization of PCL as well as PLLA soft segments.[34] This led to gelation at 37 °C with weak gel modulus (G') below 3500 Pa. Moreover, the initial gel was not firm enough for cell printing and layer-by-layer deposition. The current study further introduced amphiphilic blocks containing PEO. The presence of the amphiphilic PLLA–PEO blocks significantly promoted the self-assembly and raised the gel modulus to 6500 Pa, which was strong enough for layer-by-layer deposition. We propose that the hydrogen bonding and hydrophilicity of PEO block segregated the PCL soft segment and increased its crystallinity.[35] The crystallinity of PCL segment and its low T_g allowed gelation to occur near body temperature. Meanwhile, excessive PEO may prevent PCL from crystallization,[36] as probably was the case of PCL80LEL20. Although PEO segments may prolong the gelation time by preventing coagulation,[37] the chain mobility in PU NPs increases as the temperature increases, which explains the fast gelation near body temperature. In addition, the PEO segment moves toward surface after water removal. The very hydrophilic surface of PCL90LE10 films (contact angle $\approx$ 24°) may serve as nonfouling surface for other medical applications.

The fractal dimension of the PCL90LE10 gel at 37 °C was 2.6, as determined by the SAXS. This value was close to that predicted for a percolation cluster (~2.5).[38] A common biopolymer, gelatin, was reported to have a $d_f \approx 2.5$.[30] Gelatin has been employed as a cell-printing material. For this purpose, gelatin that is soluble at 37 °C could be cured by adding toxic cross-linkers such as glutaraldehyde.[39] Regarding the methacrylated gelatin, the toxicity to MSCs arises from the free radical generated during the photoinitiation process.[40] We observed that gelatin gel cross-linked by a less toxic chemical cross-linker (carbodiimide) resulted in cell viability lower than that of 25% PU gel even after 72 h (Figure S3). Most body-temperature-curable gels involve the block copolymers of PEO and propylene oxide (PPO) or those of PEO and PLA. The former family was nonbiodegradable. The latter family may have acidic degradation products, and the gel may be too weak (~1000 Pa) to be printed.[41] The advantage of PCL90LE10 as a printing ink is its low viscosity at room temperature and rapid irreversible gelation near body temperature. This process is somewhat similar to gelation of collagen as reconstituted fibers. When the PU NP dispersion was mixed with cells at a solid content of 25%, cells kept proliferating after printing. This confirmed the good cytocompatibility of the PU NP dispersion and gel. For concentrations lower than 25%, the hydrogel was too soft, and the extruded fiber became discontinuous. If the PU NPs was further diluted to 20%, then gelation occurred very slowly, and the gel collapsed after stacking. Therefore, the polymer at 25–30% was the most suitable for printing. Rheological profiles for PU NP dispersion at various solid contents are portrayed in Figure S4 and summarized in Table S1. To be a proper candidate for 3D-cell-printing ink, the ink must have good cytocompatibility as well as physicochemical and mechanical properties. In this study, the viability and proliferation of MSCs cultured in 25% PU gel were higher than those of MSCs cultured in 30% PU gel. All gels (30%) have swelling ratio >200%. The swelling ratio of 30% PCL90LE10 gel was determined to be 209.2 ± 1.5%, whereas that of 25% PCL90LE10 gel was swollen to about 300%. However, the different cell survival and cell growth rates are more likely due to the difference in stiffness rather than swelling ratio of the hydrogels.[42,43]

In addition to the proper modulus mentioned above, the ink must solidify in order to be stacked layer by layer (Figure S5). Moreover, the ink must prevent cells from shear damage during printing. The structure of the gel should remain integrated after printing.[44] The biodegradable PU NP dispersion/gel developed in this study has low viscosity at 25 °C to facilitate mixing with cells and quick gelation near body temperature. These features may make the PU NP dispersion/gel a novel family of candidates for 3D cell printing.

5. CONCLUSIONS

This study employed a waterborne process to successfully prepare PU NP dispersion based on PCL diol and one of the three different amphiphilic copolymer diols as the soft segment. PU with soft segment containing 10–20% amphiphilic blocks demonstrated significantly different properties from PU with 100% PCL diol as the soft segment. Among them, PCL90LE10 had the lowest surface contact angle of about 24° and the highest degree of crystallinity near 14%. ATR-IR spectra showed that the surface was enriched with EO blocks, which may increase the extent of microphase separation. The dispersion had low viscosity below room temperature. When the temperature was raised to close to body temperature, the dispersion reached the gel point after ~170 s and had good gel modulus of ~6.5 kPa in 20 min. The proper dispersion of solid content (25–30%) could be printed together with stem cells at 37 °C. Cells proliferated in the deposited layers. The PU hydrogel is a smart, thermoresponsive gel near body temperature and a novel 3D-printing ink for layer-by-layer cell/tissue printing.

■ ASSOCIATED CONTENT

Supporting Information

The Supporting Information is available free of charge on the ACS Publications website at DOI: 10.1021/acsami.5b10697.

Macroscopic images of the gelation of PU NPs, the SAXS data of PCL87LE13, cell viability of PU gel and chemical gel, rheological profiles at various solid contents, and gross appearance of 3D-printed hydrogel. (PDF)

Video showing 3D printing of hydrogel. (AVI)

■ AUTHOR INFORMATION

Corresponding Author

*Phone: (886) 2-33665313. Fax: (886) 2-33665237. E-mail: shhsu@ntu.edu.tw.

Notes

The authors declare no competing financial interest.

■ ACKNOWLEDGMENTS

This research was supported by the Program for Additive Manufacturing (MOST 103-2218-E-002-016), Ministry of

DOI: 10.1021/acsami.5b10697
ACS Appl. Mater. Interfaces 2015, 7, 27613–27623

Science and Technology, Taiwan, R.O.C, and the University Cutting-Edge Steering Research Project (NTU-CESRP-103R104941).

REFERENCES

(1) Eceiza, A.; Martin, M. D.; de la Caba, K.; Kortaberria, G.; Gabilondo, N.; Corcuera, M. A.; Mondragon, I. Thermoplastic Polyurethane Elastomers Based on Polycarbonate Diols with Different Soft Segment Molecular Weight and Chemical Structure: Mechanical and Thermal Properties. *Polym. Eng. Sci.* **2008**, *48*, 297–306.

(2) Oertel, G. *Polyurethane Handbook*, 2nd ed.; Hanser Publishers: New York, 1985.

(3) Kim, B. K.; Lee, J. C. Waterborne Polyurethanes and Their Properties. *J. Polym. Sci., Part A: Polym. Chem.* **1996**, *34*, 1095–1104.

(4) Madbouly, S. A.; Otaigbe, J. U. Rheokinetics of Thermal-Induced Gelation of Waterborne Polyurethane Dispersions. *Macromolecules* **2005**, *38*, 10178–10184.

(5) Ehleben, C. M.; Randolph May, S.; Still, J. M., Jr. Pain. Associated with an Adherent Polyurethane Wound Dressing. *Burns* **1985**, *12*, 122–126.

(6) Cherng, J. Y.; Hou, T. Y.; Shih, M. F.; Talsma, H.; Hennink, W. E. Polyurethane-Based Drug Delivery Systems. *Int. J. Pharm.* **2013**, *450*, 145–162.

(7) Hamley, I. W. *The Physics of Block Copolymers*; Oxford University Press: Oxford, U.K., 1999.

(8) Pranamuda, H.; Tsuchii, A.; Tokiwa, Y. Poly (L-lactide)-Degrading Enzyme Produced by Amycolatopsis sp. *Macromol. Biosci.* **2001**, *1*, 25–29.

(9) Dische, D. E.; Eisenberg, A. Polymer Vesicles. *Science* **2005**, *297*, 967–973.

(10) Hu, Y.; Jiang, X.; Ding, Y.; Zhang, L.; Yang, C.; Zhang, J.; Chen, J.; Yang, Y. Preparation and Drug Release Behaviors of Nimodipine-Loaded Poly(caprolactone)-Poly(ethylene oxide)-Polylactide Amphiphilic Copolymer Nanoparticles. *Biomaterials* **2003**, *24*, 2395–2404.

(11) Ahmed, F.; Discher, D. E. Self-Porating Polymersomes of PEG–PLA and PEG–PCL: Hydrolysis-Triggered Controlled Release Vesicles. *J. Controlled Release* **2004**, *96*, 37–53.

(12) Jeong, B.; Bae, Y. H.; Kim, S. W. Drug Release from Biodegradable Injectable Thermosensitive Hydrogel of PEG–PLGA–PEG Triblock Copolymers. *J. Controlled Release* **2000**, *63*, 155–163.

(13) Riley, T.; Stolnik, S.; Heald, C. R.; Xiong, C. D.; Garnett, M. C.; Illum, L.; Davis, S. S.; Purkiss, S. C.; Barlow, R. J.; Gellert, P. R. Physicochemical Evaluation of Nanoparticles Assembled from Poly-(lactic acid)-Poly(ethylene glycol) (PLA-PEG) Block Copolymers as Drug Delivery Vehicles. *Langmuir* **2001**, *17*, 3168–3174.

(14) Mert, O.; Doganci, E.; Erbil, H. Y.; Demir, A. S. Surface Characterization of Poly(L-lactic acid)–Methoxy Poly(ethylene glycol) Diblock Copolymers by Static and Dynamic Contact Angle Measurements, FTIR, and ATR-FTIR. *Langmuir* **2008**, *24*, 749–757.

(15) Saha, S. K.; Tsuji, H. Enhanced Crystallization of Poly(L-lactide-*co*-ε-caprolactone) in the Presence of Water. *J. Appl. Polym. Sci.* **2009**, *112*, 715–720.

(16) Carlsen, A.; Lecommandoux, S. Self-Assembly of Polypeptide-Based Block Copolymer Amphiphiles. *Curr. Opin. Colloid Interface Sci.* **2009**, *14*, 329–339.

(17) Wei, Y. Y.; Luo, Y. W.; Li, B. F.; Li, B. G. Polyurethane Acrylate Microgel Synthesized by Emulsion Polymerization Using Unsaturated Self-Emulsified Polymer. *Colloid Polym. Sci.* **2006**, *284*, 1171–1178.

(18) Hsu, S.h; Hung, K. C.; Lin, Y. Y.; Su, C. H.; Yeh, H. Y.; Jeng, U. S.; Lu, C. Y.; Dai, S. A.; Fu, W. E.; Lin, J. C. Water-Based Synthesis and Processing of Novel Biodegradable Elastomers for Medical Applications. *J. Mater. Chem. B* **2014**, *2*, 5083–5094.

(19) Ding, M.; Li, J.; Tan, H.; Fu, Q. Self-Assembly of Biodegradable Polyurethanes for Controlled Delivery Applications. *Soft Matter* **2012**, *8*, 5414–5428.

(20) Murphy, S. V.; Atala, A. 3D Bioprinting of Tissues and Organs. *Nat. Biotechnol.* **2014**, *32*, 773–785.

(21) Singh, V.; Tiwari, M. Structure-Processing-Property Relationship of Poly(Glycolic Acid) for Drug Delivery Systems 1:Synthesis and Catalysis. *Int. J. Polym. Sci.* **2010**, *2010*, 1–23.

(22) Hung, K. C.; Tseng, C. S.; Hsu, S.h. Synthesis and 3D Printing of Biodegradable Polyurethane Elastomer by a Water-Based Process for Cartilage Tissue Engineering Applications. *Adv. Healthcare Mater.* **2014**, *3*, 1578–1587.

(23) Chen, J.; Zeng, F.; Wu, S.; Zhao, J.; Chen, Q.; Tong, Z. Reversible Fluorescence Modulation through Energy Transfer with ABC Triblock Copolymer Micelles as Scaffolds. *Chem. Commun.* **2008**, *43*, 5580–5582.

(24) Li, S. Synthesis Bioresorbable Hydrogels Prepared through Stereocomplexation between Poly(L-lactide) and Poly(D-lactide) Blocks Attached to Poly(ethylene glycol). *Macromol. Biosci.* **2003**, *3*, 657–661.

(25) Hu, S. G.; Liu, H. J. Structural Analysis and Degradation Behavior in Polyethylene glycol/ Poly (L-Lactide) Copolymers. *J. Appl. Polym. Sci.* **1994**, *51*, 473–482.

(26) Hsu, S.h.; Huang, T. B.; Cheng, S. J.; Weng, S. Y.; Tsai, C.-L.; Tseng, C.-S.; Chen, D. C.; Liu, T.-Y.; Fu, K.-Y.; Yen, B. L. Chondrogenesis from Human Placenta-Derived Mesenchymal Stem Cells in Three-Dimensional Scaffolds for Cartilage Tissue Engineering. *Tissue Eng., Part A* **2011**, *17*, 1549–1560.

(27) Popelka, S.; Machová, L.; Rypácek, F. Adsorption of Poly(ethylene oxide)–*Block*–Polylactide Copolymers on Polylactide as Studied by ATR-FTIR Spectroscopy. *J. Colloid Interface Sci.* **2007**, *308*, 291–299.

(28) Hsieh, Y. T.; Nurkhamidah, S.; Woo, E. M. Lamellar Orientation and Interlamellar Cracks in Co-Crystallized Poly(ethylene oxide)/ Poly(L-lactic acid) Blend. *Polym. J.* **2011**, *43*, 762–769.

(29) Jeng, U. S.; Liu, W. J.; Lin, T. L.; Wang, L. Y.; Chiang, L. Y. Fractal Structure of Polyhydroxylated Fullerenes in Water Solution. *Fullerene Sci. Technol.* **1999**, *7*, 599–608.

(30) Hsu, S.h; Jamieson, A. M. Viscoelastic Behaviour at the Thermal Sol-Gel Transition of Gelatin. *Polymer* **1993**, *34*, 2602–2608.

(31) Yan, R. X. *Water-Soluble Polymers*; Chemical Industry Press: Beijing, 1998.

(32) Beran, J. A.; Kevan, L. Semiempirical Calculation of Molecular Polarizabilities and Diamagnetic Susceptibilities of Fluorocarbons, Substituted Fluorocarbons, Ethers, Esters, Ketones, and Aldehydes. *J. Phys. Chem.* **1969**, *73*, 3860–3866.

(33) Loera, A. G.; Cara, F.; Dumon, M.; Pascault, J. P. Porous Epoxy Thermosets Obtained by a Polymerization-Induced Phase Separation Process of a Degradable Thermoplastic Polymer. *Macromolecules* **2002**, *35*, 6291–6297.

(34) Ou, C. W.; Su, C. H.; Jeng, U. S.; Hsu, S.h. Characterization of Biodegradable Polyurethane Nanoparticles and Thermally Induced Self-Assembly in Water Dispersion. *ACS Appl. Mater. Interfaces* **2014**, *6*, 5685–5694.

(35) Cakić, S. M.; Ristić, I. S.; Krakovský, I.; Stojiljković, D. T.; Belský, P.; Kollová, L. Crystallization and Thermal Properties in Waterborne Polyurethane Elastomers: Influence of Mixed Soft Segment Block. *Mater. Chem. Phys.* **2014**, *144*, 31–40.

(36) Ding, M.; Qian, Z.; Wang, J.; Li, J.; Tan, H.; Gu, Q.; Fu, Q. Effect of PEG Content on the Properties of Biodegradable Amphiphilic Multiblock Poly(ε-caprolactone urethane)s. *Polym. Chem.* **2011**, *2*, 885–892.

(37) Riley, T.; Govender, T.; Stolnik, S.; Xiong, C. D.; Garnett, M. C.; Illum, L.; Davis, S. S. Colloidal Stability and Drug Incorporation Aspects of Micellar-Like PLA–PEG Nanoparticles. *Colloids Surf., B* **1999**, *16*, 147–159.

(38) Rammal, R.; Toulouse, G. Random Walks on Fractal Structures and Percolation Clusters. *J. Phys., Lett.* **1983**, *44*, 13–22.

(39) Jiao, Y.; Ma, S.; Li, J.; Shan, L.; Yang, Y.; Li; Chen, J. M. The Influences of N-acetyl Cysteine (NAC) on the Cytotoxicity and Mechanical Properties of Poly-Methylmethacrylate (PMMA)-Based Dental Resin. *PeerJ* **2015**, *3*, e868.

(40) Lin, F. H.; Yao, C. H.; Sun, J. S.; Liu, H. C.; Huang, C.-W. Biological Effects and Cytotoxicity of the Composite Composed by

DOI: 10.1021/acsami.5b10697
ACS Appl. Mater. Interfaces 2015, 7, 27613–27623

Tricalcium Phosphate and Glutaraldehyde Cross-Linked Gelatin. *Biomaterials* **1998**, *19*, 905–917.
(41) Li, S.; El Ghzaoui, A. E.; Dewinck, E. Rheology and Drug Release Properties of Bioresorbable Hydrogels Prepared from Polylactide Poly(ethylene glycol) Block Copolymers. *Macromol. Symp.* **2005**, *222*, 23–36.
(42) Liu, S. Q.; Tian, Q.; Hedrick, J. L.; Po Hui, J. H.; Rachel Ee, P. L.; Yang, Y. Y. Biomimetic Hydrogels for Chondrogenic Differentiation of Human Mesenchymal Stem Cells to Neocartilage. *Biomaterials* **2010**, *31*, 7298–7307.
(43) Kim, J.; Park, Y.; Tae, G.; Lee, K. B.; Hwang, C. M.; Hwang, S. J.; Kim, I. S.; Noh, I.; Sun, K. Characterization of Low-Molecular-Weight Hyaluronic Acid-Based Hydrogel and Differential Stem Cell Responses in the Hydrogel Microenvironments. *J. Biomed. Mater. Res., Part A* **2009**, *88A*, 967–975.
(44) Chung, H. Y.; Naficy, S.; Yue, Z.; Kapsa, R.; Quigley, A.; Moulton, S.; Wallace, G. G. Bio-Ink Properties and Printability for Extrusion Printing Living Cells. *Biomater. Sci.* **2013**, *1*, 763–773.

DOI: 10.1021/acsami.5b10697
ACS Appl. Mater. Interfaces 2015, 7, 27613–27623